Polyhedron 225 (2022) 116079

Contents lists available at ScienceDirect

Polyhedron

journal homepage: www.elsevier.com/locate/poly

# Ni(II), Cu(II) and Zn(II) complexes of functionalised thiosemicarbazone ligands: Syntheses and reactivity, characterization and structural studies

Ali A.A. Al-Riyahee [a], Peter N. Horton [b], Simon J. Coles [b], Angelo J. Amoroso [a,*], Simon J. A. Pope [a,*]

[a] School of Chemistry, Main Building, Cardiff University, Cardiff CF10 3AT Wales, UK
[b] UK National Crystallographic Service, Chemistry, Faculty of Natural and Environmental Sciences, University of Southampton, Highfield, Southampton SO17 1BJ, UK

ARTICLE INFO

*Keywords:*
Thiosemicarbazone
Transition metal complexes
Crystallography

ABSTRACT

The synthesis of two thiosemicarbazone derivatised ligands (**L1** and **L2**) was accomplished via the reaction of 1-(2-pyridinyl)ethanone hydrazone and either benzoyl or pivaloyl isothiocyanate. A range of Ni(II), Cu(II) and Zn(II) mononuclear complexes of these thiosemicarbazone ligands have been synthesized providing insight on the reactivity of the ligands. These complexes (**1**–**12**) have been characterized by high resolution mass spectrometry, IR, UV–vis., $^{1}$H and $^{13}$C NMR spectroscopies, elemental analysis and magnetic measurements. The solid-state molecular structures of eight examples were successfully determined by single crystal X-ray diffraction.

## 1. Introduction

The synthesis and structural studies of transition metal complexes of thiosemicarbazone ligands continues to attract attention.[1] This has been, in part, driven by the potential applications of bioactive thiosemicarbazones as antifungal,[2] antitumour,[3] antiviral,[4] antitubercular,[5] antibacterial,[6] and antimalarial[7] agents. Some studies have also focused upon the cytotoxic activity of thiosemicarbazones derived from 2-formylpyridine, which have shown antineoplastic [8] action against a variety of human solid tumour cell lines. The development of new herbicidal [9] and insecticidal [10] agents with novel modes of action is a continuing area of interest for those working in disciplines associated with crop protection and environmental health. [11] Here too, thiosemicarbazones have found promise, particularly those that have been developed for their antifungal properties (Scheme 1)

The study of metal complexes of thiosemicarbazone ligands[12] is relevant as the presence of the metal can significantly alter the toxicological profile and mode of action [13] of bioactive agents.[14] Metal chelation can control charge and lipophilicity and thus modulate (and promote) lipid membrane transport; integrating metal chelation into the design of these agents is, therefore, an important design tool. Very recent studies have shown the advantageous influence of copper chelation in antifungal and anti-aflatoxigenic agents based on thiosemicarbazone derivatives.[15].

Thiosemicarbazones have a rich history as ligands for different transition metal ions, [16] for example including copper, [17,18] palladium,[19] lead,[20] tin,[21] cadmium,[22] nickel,[23] platinum, [24] and even uranyl,[25] primarily due to the ability to coordinate in a number of different ways[26] via the presence of various donor atoms within their structures. Typical bonding modes occur through the sulfur donor and the hydrazinic nitrogen atoms.[27] The ease of varying the molecular structures of thiosemicarbazones has expanded their utility as ligands because additional groups can be added to create multiple sites of metal coordination providing added stability to metal complexes through the formation of chelate rings. For example, acyclic ligands such as pyruvaldehyde bis-(*N*4-methylthiosemicarbazone) (PTSM) and diacetyl-bis(*N*4-methylthiosemicarbazone) (ATSM) have been widely investigated.[28] In particular, the copper complexes of these bis(thiosemicarbazone) have been studied *in vivo* with respect to non-hypoxia or hypoxia selective cell uptake. Furthermore, $^{64}$Cu(II) radiolabelled ATSM has been extensively studied to identify hypoxic tissues using positron imaging tomography (PET)[29] although there are ongoing challenges in their clinical application [30].

The current work builds from, and relates to, our ongoing interests in the coordination chemistry of thiourea derived mixed-donor ligands and their potential application in biological disciplines. [31] Herein we present an investigation into N,N,S donor ligands based upon functionalized thiosemicarbazone species and their coordination chemistry with divalent salts, Ni(II), Cu(II) and Zn(II).

* Corresponding authors.
*E-mail addresses:* amorosoaj@cardiff.ac.uk (A.J. Amoroso), popesj@cardiff.ac.uk (S. J. A. Pope).

https://doi.org/10.1016/j.poly.2022.116079
Received 15 June 2022; Accepted 1 August 2022
Available online 5 August 2022

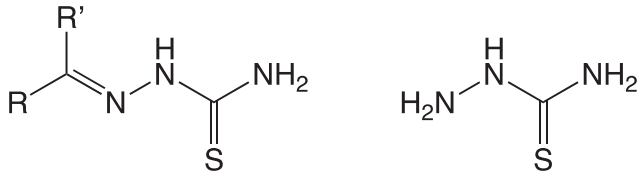

**Scheme 1.** The structures of a thiosemicarbazone (left) core and thiosemicarbazide.

## 2. Results and discussion

### 2.1. Synthesis and characterisation of the ligands

The ligands were obtained in two synthetic steps (see Experimental section for details). Firstly, reaction between benzoyl or pivaloyl chloride with potassium thiocyanate yielded the corresponding benzoyl or pivaloyl isothiocyanate. The ligands were then prepared from the reaction of the acylisothiocyanate with 1-(2-pyridinyl)ethanone hydrazone (Scheme 2) to give the thiosemicarbazone derived ligands, **L1** and **L2**, respectively. These species were isolated as air stable, yellow solids.

The ligands were firstly characterised by $^{1}$H and $^{13}$C NMR spectroscopy (see experimental section for details). The $^{1}$H NMR spectra for the ligands show that the two distinct N*H* hydrogens appear downfield with two singlet signals at 13.72 and 9.20 ppm (**L1**) and 13.58 and 8.62 ppm (**L2**). Singlets at 2.56 and 2.49 ppm were also assigned to the methyl groups in **L1** and **L2**, respectively, and **L2** showed an additional upfield singlet at 1.30 ppm due to the pivaloyl group. In addition, **L1** showed multiple peaks around 7.30–8.59 ppm, which are attributed to the different aromatic protons of the benzamide and pyridyl rings.

The $^{13}$C NMR spectra of **L1** and **L2** showed the expected resonances observed around 122.2–158.3 ppm and 121.9–157.8 ppm, respectively, which are assigned to the aromatic carbons and at 12.96 and 12.26 ppm, respectively, due to the carbon of the methyl group. Downfield signals that appeared at 167.2 (**L1**) and 177.3 ppm (**L2**) were assigned attributed to the carbonyl group group, and the characteristic C═S groups were identified 177.2 and 179.2 ppm for **L1** and **L2**, respectively. Both ligands also gave satisfactory high resolution mass spectrometry (HRMS) results and supporting IR spectroscopy data was also obtained, which is discussed later in the context of the isolated complexes.

### 2.2. Synthesis and characterisation of the complexes

The scope of the ligand reactivity and coordination chemistry is shown in Schemes 3 and 4. Reactions between **L1** and $Cu(ClO_4)_2{\cdot}6H_2O$ were investigated using both 1:1 and 2:1 stoichiometries using a solvent mixture of DMF/water at room temperature. The analytical, spectral and crystallographic data indicated the formation of [Cu(**L1**$^{-}$)(MeCN)($H_2O$)]($ClO_4$) (**1**) and [Cu(**L1**)$_2$]($ClO_4$)$_2$ (**2**) (Scheme 2) both of which are divalent copper species. In each case the ligand coordinates in a tridentate NˆNˆS fashion. It is noteworthy that complex **1** includes the ligand in its deprotonated and thus anionic state.[32] The Cu(II) complexes with **L1** were partially soluble in acetone, acetonitrile, and alcohols, but insoluble in less polar solvents such as $CHCl_3$, DCM, *n*-hexane. The Cu(II) complexes with **L2** were completely soluble in a range of solvents such as acetone, acetonitrile, alcohol, ethyl acetate, $CHCl_3$, and DCM.

The Ni(II) complexes were isolated and demonstrated that either 1:1 or 2:1 ratios of L:Ni could be obtained. For example, complex **3**, which was obtained by reaction of **L1** and $Ni(ClO_4)_2{\cdot}6H_2O$ in a 2:1 M ratio at 50 °C, revealed a six coordinate complex with each neutral ligand coordinating in a tridentate manner, whereas four coordinate complex **5** has the formulation [Ni(**L1**$^{-}$)Cl]. Similar reactivity of **L1** was noted with the different Zn(II) salts: complex **4** is analogous to **3**, and complex **6**, which is neutral, has the formulation of [$ZnCl_2$(**L1**)] (note the ligand is neutral).

The reactivity of **L2** showed some differences to **L1**. Reaction between **L2** with $Cu(BF_4)_2{\cdot}6H_2O$ in both 1:1 and 2:1 stoichiometries gave Cu(II) complexes of the formulation [Cu(**L2**$^{-}$)(DMF)]$BF_4$ (**8**) and [Cu(**L2**)$_2$]($BF_4$)$_2$ (**9**). During our studies, it was noted that reactions of **L2** at room temperature often led to cleavage of the pivaloyl group. Deprotection of *N*-pivaloyl groups is often assisted by basic or reducing conditions, neither of which were expected here. Complexes **7** [Cu(**L2′**$^{-}$)(DMF)]$BF_4$, (the cleaved ligand is denoted **L2′**) and **11** [$ZnCl_2$(**L2′**)] revealed the cleaving behaviour. Reducing the reaction temperature to 0 °C appeared to inhibit ligand cleavage and therefore complexes **8**, **9** and **12** show that the integrity of the ligand can be retained in this adaption to the reaction conditions. Interestingly, reaction of **L2** with $NiCl_2$ at room temperature gave complex **10** which did not show any loss of the pivaloyl group. This may imply that the metal ion also plays a role in the sensitivity of **L2** to cleavage.

In terms of the spectroscopic characterisation, firstly IR spectroscopy was employed for the complexes due to the number of IR active functional groups (e.g. NH, C═O, C═S) within the molecular structures. The key vibrational frequencies for the ligands and complexes are highlighted in Table 1. The data for the $\nu$(C═S) absorption is notable as it shows the impact of coordination, which lowers the vibrational frequency in all cases when compared to the free ligand(s) and thus

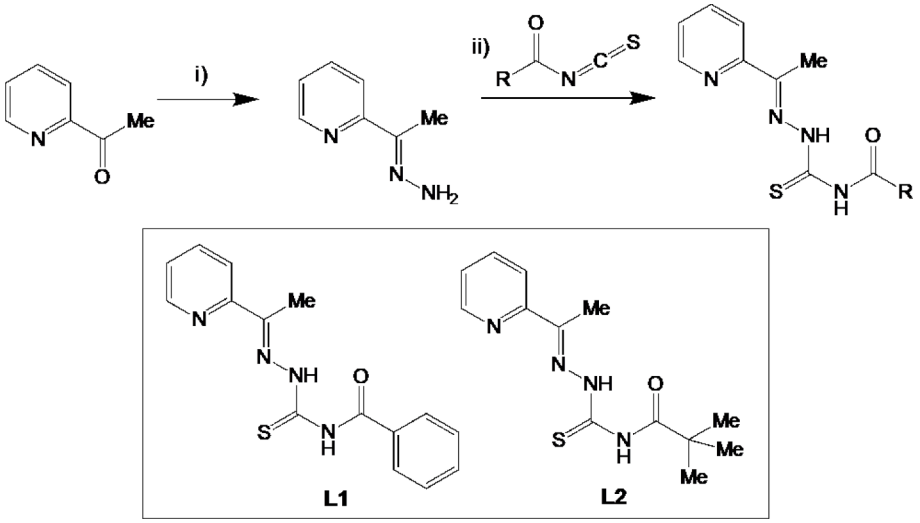


**Scheme 2.** Synthetic route to the ligands, **L1** and **L2** (shown inset). Reagents and conditions: i) $NH_2NH_2$, 24 hr, rt; ii) MeCN, reflux (**L1**) or rt (**L2**), 3 hr.

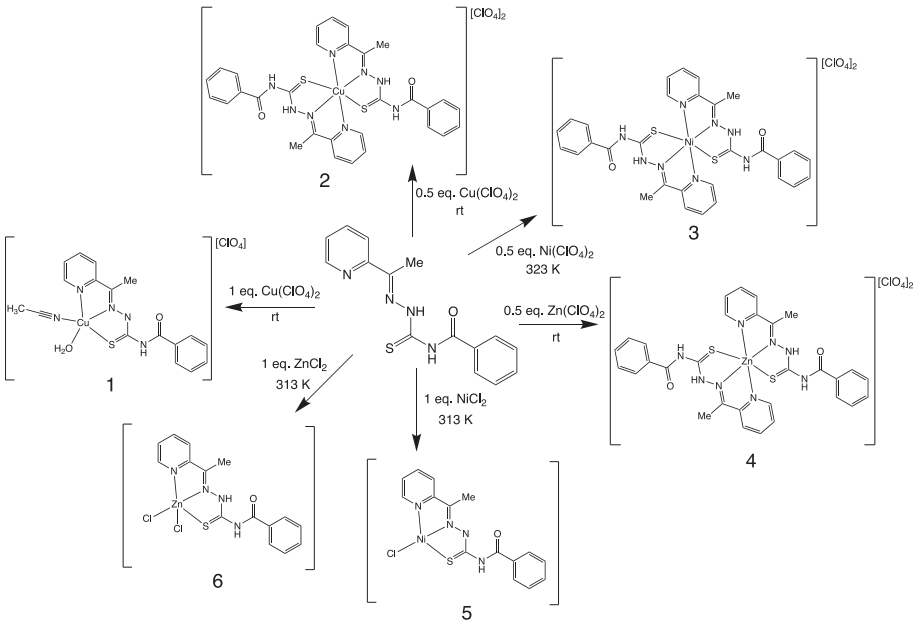


**Scheme 3.** Synthesis of the complexes **1**–**6** using **L1**.

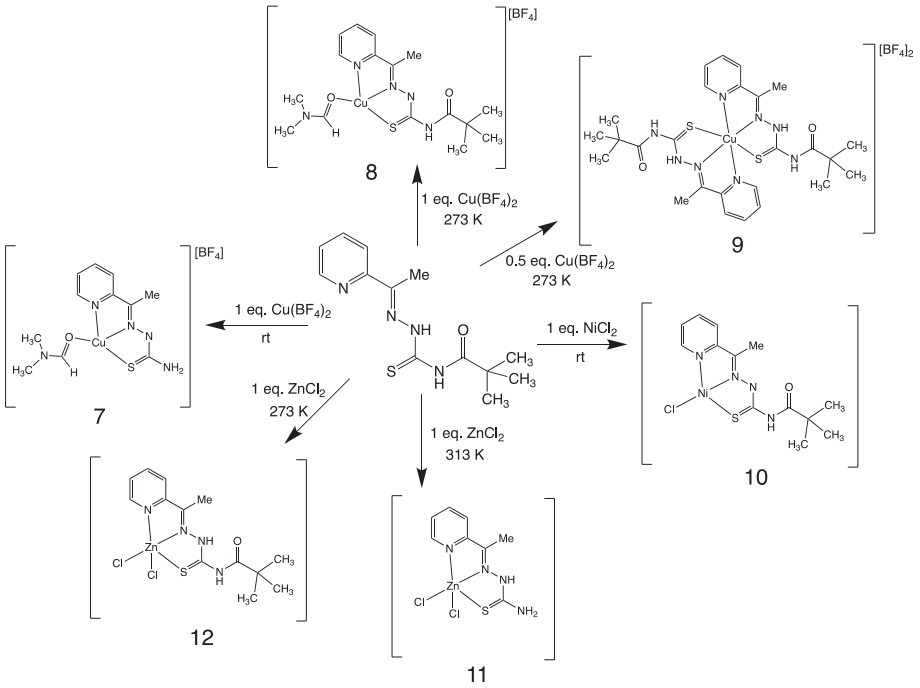


**Scheme 4.** Synthesis of the complexes **7**–**12** using **L2**.

**Table 1**
Selected infrared spectral and assignments ($cm^{-1}$) for **L1** and **L2** and the complexes (**1**–**12**).

| Compound | ν(N—H) | ν(C=O) | ν(C=S) | Compound | ν (N—H) | ν (C=O) | ν (C=S) |
|---|---|---|---|---|---|---|---|
| **L1** | 3391 | 1663 | 1332 | **L2** | 3298 | 1672 | 1371 |
| **1** | 3429 | 1660 | 1263 | **7** | 3333 | 1710 | 1325 |
| **2** | 3410 | 1662 | 1258 | **8** | 3335 | 1707, 1670 | 1322 |
| **3** | 3350 | 1660 | 1252 | **9** | 3329 | 1669 | 1330 |
| **4** | 3366 | 1663 | 1250 | **10** | 3314 | 1671 | 1337 |
| **5** | 3310 | 1664 | 1263 | **11** | 3170 | – | 1321 |
| **6** | 3279 | 1663 | 1270 | **12** | 3167 | 1670 | 1340 |

confirms coordination of this donor unit to the metal ion. For complexes **7** and **8** the coordinated DMF was confirmed by the ν(C═O) feature ca. 1710 $cm^{-1}$. The case of **11** highlights the absence of a carbonyl frequency which is consistent with cleavage of the pivaloyl group. Loss of the pivaloyl group leads to a lowering of the ν(C═S) value (**11** *vs* **12**) which is consistent with the formation of the terminal $NH_2$ group.

$^1H$ and $^{13}C$ NMR spectroscopic data were obtained for the diamagnetic Zn(II) complexes in the series and data are listed in the Experimental section. Complexes **4**, **6**, **11** and **12** were recorded in DMSO-$d_6$ and the $^1H$ NMR data showed ligand-based aromatic protons in the range 7.43–8.66 ppm and two resonances in the range 13.40–14.06 and 11.28–11.74 ppm which were assigned to the presence of N*H* environments. These two resonances are shifted downfield after complexation due to the intramolecular hydrogen bonds N—H···O which are common in thiosemicarbazone complexes. Complex **11** showed the disappearance of the aliphatic singlet signal expected for the pivaloyl group (*cf*. **L2**), indicating cleavage of this moiety. The $^{13}C$ NMR spectra obtained for the complexes showed all the expected resonances signals due to the different carbon environments. The signals observed in the range 120.6–159.2 ppm were assigned to the different aromatic carbons of the unsymmetrical thiosemicarbazone ligands. The characteristic downfield resonances due to the C═S and C═O groups were shifted compared to their corresponding free ligands, and appeared in the regions of 177.4–178.5 and 167.7–171.3 ppm, respectively in the complexes, confirming that the C═S group is coordinated to Zn(II). Again, $^{13}C$ NMR spectral data was able to confirm cleavage of the pivaloyl group in **11** through the absence of the C═O resonance.

### 2.3. X-ray crystallographic studies

Single crystals suitable for diffraction studies were isolated for eight of the complexes **1**, **5**, **6**, **7**, **8**, **10, 11** and **12**. Crystal parameters and details of the data collection and structural refinements of the complexes are presented in Tables 2 and 3 with all data collections carried out at 100 K. Further details are given in the Experimental section. All compounds crystallised in centrosymmetric space groups (i.e. one that has an inversion centre).

### 2.4. X-ray structure of [Cu(L1$^-$)($CH_3CN$)($H_2O$)]$ClO_4$ (1)

Monoclinic, lath-shaped pale green crystals of **1** were obtained by vapour diffusion of diethyl ether into an acetonitrile solution of the complex. There are 2 independent anion complexes in the asymmetric unit, that basically have the same structural features. Selected bond distances and bond angles are given in Table 4. Fig. 1 shows the Cu(II) ion is coordinated by one tridentate ligand, one acetonitrile solvent and one water molecule. The ligand is coordinating through the pyridine ring, and nitrogen and sulfur donors of the thiosemicarbazone giving two 5-membered chelate rings. The coordinated water molecule occupies the axial position of an approximately square based pyramidal geometry with coordinate bond angles from 80.77(6)-101.75(4)° and 161.99(5)-175.02(7)°. As expected, the longest coordinated bonds are the Cu-S and the axial Cu–O at 2.2797(5), 2.2802(5) and 2.3748(14), 2.3848(14) Å, respectively. A related complex [Cu(L)(pic)] (where L = pyridine-2-carbaldehyde thiosemicarbazone; pic = picolinate), has also been reported that adopts a square pyramidal coordination environment and contains very similar bond lengths (Cu–N1, Cu–N2 and Cu–S1: 2.0430(5), 1.9255(5), 2.2799(5) Å) and angles. [33] The packing diagram for **1** revealed an intermolecular hydrogen bond between the coordinated water oxygen atom and a neighbouring thiosemicarbazone hydrogen atom.

### 2.5. X-ray structures of [NiCl(L1$^-$)].DMF (5) and [NiCl(L2$^-$)] (10)

Triclinic, plate red crystals of **5** and monoclinic, lath orange crystals of **10** were obtained by vapour diffusion of diethyl ether into a DMF or acetonitrile solution of **5** and **10**, respectively. **5** crystallised as the DMF solvate, but otherwise the structures of both are closely related; the anionic form of the ligands is present in both. The Ni(II) coordination spheres are completed by a monodentate chloride and a tridentate anionic thiosemicarbazone ligand, which contributes a $N_2S$ donor set. Fig. 2 shows that the Ni(II) complexes are approximately square planar with bond angles about the metal centres ranging from 83.42(5)-97.55(4)° (**5**), 83.10(14)-95.90(10)° (**10**), and 170.57(4)-179.01(4)° (**5**), 170.44(10)-179.00(10)° (**10**). The distortions away from ideal geometry are due to the bite angle of the thiosemicarbazone ligands. Table 5 shows selected bond lengths and angles for complexes **5** and **10**. The Ni-L bond distances are very similar for **5** and **10** and are comparable to those reported for another square planar complex with a related ligands system. [34] For **5** there is also one intermolecular hydrogen bond (ca. 1.97 Å) which occurs between the solvent DMF oxygen atom and the thiosemicarbazone hydrogen atom.

### 2.6. X-ray structure of [$ZnCl_2$(L1)] (6)

Monoclinic, plate light yellow crystals of **6** were obtained by vapour

**Table 2**
Crystallographic data for complexes **1**, **5, 6** and **7**.

| Compound | 1 | 5 | 6 | 7 |
|---|---|---|---|---|
| **Chemical Formula** | $CuC_{17}H_{18}ClN_5O_6S$ | $NiC_{18}H_{20}ClN_5\ O_2S$ | $ZnC_{15}H_{14}Cl_2N_4OS$ | $CuC_{17}H_{30}BF_4N_7O_3S$ |
| **Mr. g.mol$^{-1}$** | 519.41 | 464.61 | 434.63 | 562.89 |
| **Crystal system** | Monoclinic | Triclinic | Monoclinic | Monoclinic |
| **Space group** | $P2_1/n$ | P-1 | $P2_1/c$ | $P2_1/c$ |
| **a, Å** | 15.1171(2) | 9.5200(3) | 11.6555(4) | 14.2582(4) |
| **b, Å** | 15.1732(2) | 10.0378(3) | 18.0296(4) | 23.4417(7) |
| **c, Å** | 18.4326(3) | 11.4030(4) | 8.5246(3) | 7.5036(2) |
| **α, degree** | 90° | 111.945(3)° | 90° | 90° |
| **β, degree** | 107.034(2)° | 91.731(3)° | 110.454(3)° | 101.573(3)° |
| **γ, degree** | 90° | 105.202(3)° | 90° | 90° |
| **Z** | 8 | 2 | 4 | 4 |
| **Dc. Mg/m$^3$** | 1.707 | 1.598 | 1.720 | 1.522 |
| **μ($M_O$ K α), mm$^{-1}$** | 1.363 | 1.277 | 1.916 | 1.038 |
| **Observed reflections** | 50,790 | 16,749 | 18,545 | 26,206 |
| **Unique reflections** | 9242 | 4423 | 3826 | 5601 |
| **$R_{int}$** | 0.0293 | 0.0197 | 0.0209 | 0.0681 |
| **R1 [I > 2σ<(I)]** | 0.0333 | 0.0225 | 0.0210 | 0.0703 |
| **w*R*2(all data)** | 0.0872 | 0.0563 | 0.0529 | 0.1646 |

**Table 3**
Crystallographic data for **8**, **10**, **11** and **12**.

| Compound | 8 | 10 | 11 | 12 |
|---|---|---|---|---|
| **Chemical Formula** | $CuC_{20.50}H_{34.50}BF_4N_{6.50}O_{3.50}S$ | $NiC_{13}H_{17}ClN_4$ OS | $ZnC_{11}H_{17}Cl_2N_5$ OS | $ZnC_{13}H_{18}Cl_2N_4OS$ |
| **Mr. g.mol$^{-1}$** | 610.45 | 371.52 | 403.62 | 414.64 |
| **Crystal system** | Monoclinic | Monoclinic | Triclinic | Monoclinic |
| **Space group** | $P2_1/n$ | $P2_1/m$ | P-1 | $P2_1/c$ |
| **a, Å** | 6.59390(10) | 8.4898(5) | 7.4149(6) | 10.8879(2) |
| **b, Å** | 25.9958(5) | 6.7122(5) | 9.2264(6) | 8.5673(2) |
| **c, Å** | 31.1516(5) | 13.6507(9) | 11.9695(7) | 18.5503(4) |
| **α, degree** | 90° | 90° | 101.691(5)° | 90° |
| **β, degree** | 91.328(2)° | 101.988(6)° | 95.685(6)° | 101.544(2)° |
| **γ, degree** | 90° | 90° | 91.157(5)° | 90° |
| **Z** | 8 | 2 | 2 | 4 |
| **Dc. Mg/m$^3$** | 1.519 | 1.622 | 1.681 | 1.625 |
| **μ($M_O$ K α), mm$^{-1}$** | 0.963 | 1.590 | 2.011 | 1.892 |
| **Observed reflections** | 13,726 | 8191 | 5586 | 21,892 |
| **Unique reflections** | 13,726 | 1888 | 5586 | 3880 |
| **$R_{int}$** | N/A* | 0.0501 | N/A* | 0.0292 |
| **R1 [I > 2σ<(I)]** | 0.0555 | 0.0430 | 0.0724 | 0.0212 |
| **w*R*2(all data)** | 0.1150 | 0.1168 | 0.2129 | 0.0499 |

*Integrated as non-merohedral twins, so no Rint value. For further info, please see CIFs

**Table 4**
Selected bond lengths (Å) and bond angles (°) for complex **1**.

| Bond length (Å) | | | |
|---|---|---|---|
| Cu1–N2 | 1.9483(15) | Cu1–S1 | 2.2802(5) |
| Cu1–N21 | 1.9520(16) | Cu1–O21 | 2.3848(14) |
| Cu1–N1 | 2.0336(16) | | |
| Cu2–N32 | 1.9496(16) | Cu2–S31 | 2.2797(5) |
| Cu2–N51 | 1.9574(16) | Cu2–O51 | 2.3748(13) |
| Cu2–N31 | 2.0328(16) | | |
| Bond Angles (°) | | | |
| N2–Cu1–N21 | 175.02(7) | N1–Cu1–S1 | 161.99(5) |
| N2–Cu1–N1 | 80.77(6) | N2–Cu1–O21 | 89.41(6) |
| N21–Cu1–N1 | 98.97(7) | N21–Cu1–O21 | 95.55(6) |
| N2–Cu1–S1 | 84.57(5) | N1–Cu1–O21 | 88.56(5) |
| N21–Cu1–S1 | 94.73(5) | S1–Cu1–O21 | 101.75(4) |
| N32–Cu2–N51 | 174.94(7) | N31–Cu2–S31 | 163.62(5) |
| N32–Cu2–N31 | 80.94(6) | N32–Cu2–O51 | 89.00(6) |
| N51–Cu2–N31 | 98.04(7) | N51–Cu2–O51 | 95.94(6) |
| N32–Cu2–S31 | 84.76(5) | N31–Cu2–O51 | 88.76(5) |
| N51–Cu2–S31 | 95.50(5) | S31–Cu2–O51 | 98.98(4) |

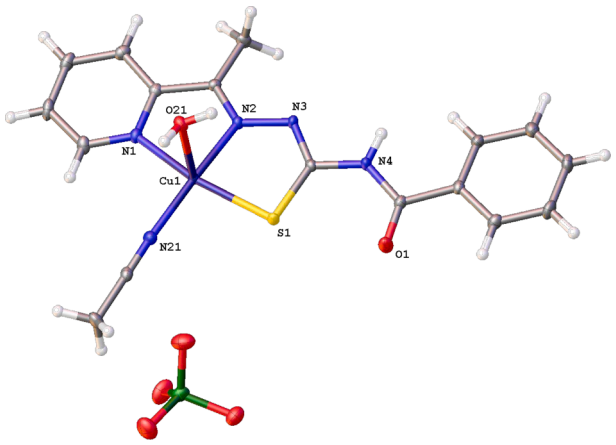


**Fig. 1.** Structure of complex **1**. Ellipsoids are drawn at 50% probability.

diffusion of diethyl ether into a DMF solution of the complex. The crystallographic data and the final refinement details are listed in Table 2 and selected bond distances and bond angles are given in Table 6. Fig. 3 shows that the Zn(II) centre is coordinated by one tridentate ligand and two chloride ions. The complex adopts a geometry that is best described as spherical square pyramidal (using SHAPE analysis) [35] with bond angles about the metal centre ranging from 72.97(5)-111.375(15)° and 96.550(13)-143.90(3)°. The more acute of these angles is associated with the bond angles between the three donors of the tridentate ligand. The bond lengths that describe the coordination sphere are comparable to a related complex [$ZnCl_2$(Hatsc)] (where Hatsc = 2-acetylpyridine(thiosemicarbazone)) reported by Nomiya *et al,* which exhibited comparable coordinative bond lengths. [36] There are two types of hydrogen bonds (intramolecular N3–H3…O1, and intermolecular N4–H4…Cl1 at about 1.87 and 2.73 Å, respectively) in complex **6** indicating that intraligand forces may rigidify the complex.

### *2.7. X-ray structures of [Cu(L2$^{\cdot-}$)(DMF)]$BF_4$.2DMF (7) and [Cu(L2$^-$)(DMF)]$BF_4$.1.5 DMF (8)*

Monoclinic, dark green crystals of **7** and **8** were obtained by vapour diffusion of diethyl ether into a DMF solution of the respective complex; both structures were obtained as the DMF solvates. For **8**, there are two independent anion complexes in the asymmetric unit, that basically have the same structural features. Selected bond distances and bond angles are given in Table 7. The two structures are very closely related, principally differing only by the absence (**7**) or retention (**8**) of the pivaloyl group. The molecular structure of **7** is shown in Fig. 4 and clearly shows the ligand has been cleaved, with a loss of the pivaloyl group which results in an $NH_2$ group, and is anionic. For **8**, the pivaloyl group is retained, but again the ligand is deprotonated and thus anionic. In both cases the structures reveal one thiosemicarbazone ligand and one DMF solvent are coordinated to the Cu(II) ion giving a 4-coordinate, approximately square planar complex; a $BF_4$ counter anion balances the charge of the cationic complex units. Bond angles and lengths in complex **7** are in closest agreement with those in a related square planar thiosemicarbazone complex of Cu(II) reported by Richardson *et al.* [37] **7** shows different intermolecular H-bonding interactions that manifest between the $NH_2$ group and DMF oxygen atom and a $BF_4$ anion.

### *2.8. X-ray structures of [$ZnCl_2$(L2′)].DMF (11) and [$ZnCl_2$(L2)] (12)*

Plate, yellow crystals of **11** and **12** were obtained by vapour diffusion of diethyl ether into a DMF solution of the complexes. Selected bond distances and bond angles are given in Table 8. As with **7** and **8**, these complexes primarily differ through the structure of the ligand. Fig. 5 shows that in **11**, cleavage of the pivaloyl group has occurred and the

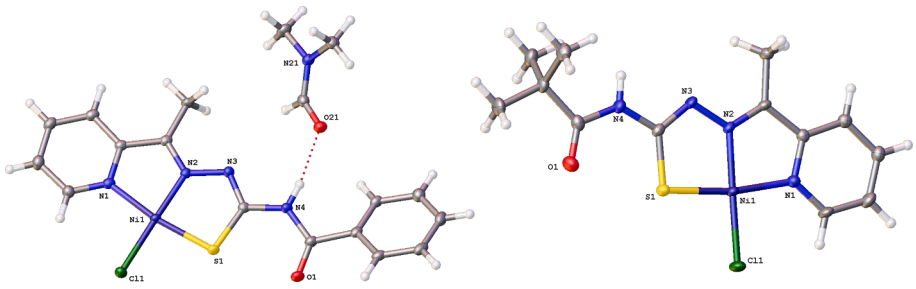


**Fig. 2.** Structures of complexes **5** (left) and **10** (right). Ellipsoids are drawn at 50% probability.

**Table 5**
Selected bond lengths (Å) and bond angles (°) for complexes **5** and **10**.

| Bond length (Å) | **5** | **10** |
|---|---|---|
| Ni1–N2 | 1.8396(11) | 1.843(3) |
| Ni1–N1 | 1.9341(15) | 1.929(3) |
| Ni1–S1 | 2.1463(4) | 2.1552(11) |
| Ni1–Cl1 | 2.1581(4) | 2.1666(11) |
| Bond Angles (°) | | |
| N2–Ni1–N1 | 83.42(5) | 83.10(14) |
| N2–Ni1–S1 | 87.25(4) | 87.34(10) |
| N1–Ni1–S1 | 170.57(4) | 170.44(10) |
| N2–Ni1–Cl1 | 179.01(4) | 179.00(10) |
| N1–Ni1–Cl1 | 97.55(4) | 95.90(10) |
| S1–Ni1–Cl1 | 91.765(18) | 93.72(4) |

**Table 6**
Selected bond lengths (Å) and bond angles (°) for complex **6**.

| Bond length (Å) | | | |
|---|---|---|---|
| Zn1–N1 | 2.1334(12) | Zn1–Cl1 | 2.2865(4) |
| Zn1–N2 | 2.1867(12) | Zn1–S1 | 2.5135(4) |
| Zn1–Cl2 | 2.2655(4) | | |
| Bond Angles (°) | | | |
| N1–Zn1–N2 | 72.97(5) | Cl2–Zn1–Cl1 | 111.375(15) |
| N1–Zn1–Cl2 | 96.59(3) | N1–Zn1–S1 | 143.90(3) |
| N2–Zn1–Cl2 | 143.07(3) | N2–Zn1–S1 | 76.37(3) |
| N1–Zn1–Cl1 | 101.42(3) | Cl2–Zn1–S1 | 96.550(13) |
| N2–Zn1–Cl1 | 105.44(3) | Cl1–Zn1–S1 | 104.751(14) |

ligand acts as a neutral tridentate donor; two additional chloride ions are present in the the coordination sphere. For **12**, no such cleavage is evident and the ligand form is retained; the coordination environment for Zn(II) is comparable to **11**. In both cases the Zn(II) adops a 5-coordinate arrangement that might be described as a very distorted trigonal bipyramidal geometry for **11** (although both are closest to spherical square based pyramidal [38]) with typical bond angles about the metal centre ranging from 73.3(3)-115.45(8)° and 110.4(2)-150.79(19)° (**11**) and 72.37(5)-116.541(15)° and 104.74(3)-138.45(3)° (**12**). The M−L bond lengths in both structures are similar and are also comparable to the literature on related systems, for example [Zn(triapine)$Cl_2$] (triapine = 3-aminopyridine-2-carboxaldehyde thiosemicarbazone) reported by Keppler *et al.* [39] However, it is noteworthy that the Zn-S bond length is slightly shorter in **11**, which may be due to the absence of the electron withdrawing *N*-pivaloyl group. As with the other structures there are several hydrogen bonding interactions that are evident, all of which are intermolecular in nature. One of these interactions occurs between the DMF oxygen atom and the terminal $NH_2$ group (ca. 1.94 Å) and other interactions between the choride ligands and the thiourea hydrogen atom (ca. 2.44 and 2.46 Å, respectively) were noted.

### 2.9. *UV–vis. Spectroscopic studies of the complexes*

The electronic spectra of the ligands **L1** and **L2** and their complexes with Cu(II), Ni(II) and Zn(II) ions were recorded in DMF solution at room temperature and the data are collected in Table 9 and the Experimental section. Firstly, the analysis of the free ligands revealed intense absorption maxima in the UV region at 287 (14500) and 345 (10800) for **L1** and 270 (21800) and 337 nm (23300 $M^{-1}cm^{-1}$) in **L2**. These strong

**Table 7**
Selected bond lengths (Å) and bond angles (°) for complexes **7** and **8**.

| Bond lengths (Å) **7** | | | **8** | | |
|---|---|---|---|---|---|
| Cu1–O11 | 1.956 (3) | Cu1–O16 | 1.940 (2) | Cu1–O36 | 1.944 (2) |
| Cu1–N2 | 1.961 (4) | Cu1–N2 | 1.946 (3) | Cu1–N22 | 1.950 (3) |
| Cu1–N1 | 2.026 (4) | Cu1–N1 | 2.011 (3) | Cu1–N21 | 2.004 (3) |
| Cu1–S1 | 2.2842 (11) | Cu1–S1 | 2.2585 (9) | Cu21–S21 | 2.2573 (9) |
| Bond Angle **7** | | **8** | | | |
| O11–Cu1–N2 | 169.27 (13) | O16–Cu1–N2 | 174.26 (11) | O36–Cu21–N22 | 173.88 (11) |
| O11–Cu1–N1 | 91.85 (13) | O16–Cu1–N1 | 93.85 (11) | O36–Cu21–N21 | 94.00 (11) |
| N2–Cu1–N1 | 80.91 (14) | N2–Cu1–N1 | 80.47 (11) | N22–Cu21–N21 | 80.87 (12) |
| O11–Cu1–S1 | 100.55 (9) | O16–Cu1–S1 | 100.17 (7) | O36–Cu21–S21 | 100.12 (7) |
| N2–Cu1–S1 | 83.98 (11) | N2–Cu1–S1 | 85.45 (9) | N22–Cu21–S21 | 85.02 (8) |
| N1–Cu1–S1 | 157.80 (10) | N1–Cu1–S1 | 165.62 (8) | N21–Cu21–S21 | 165.88 (9) |

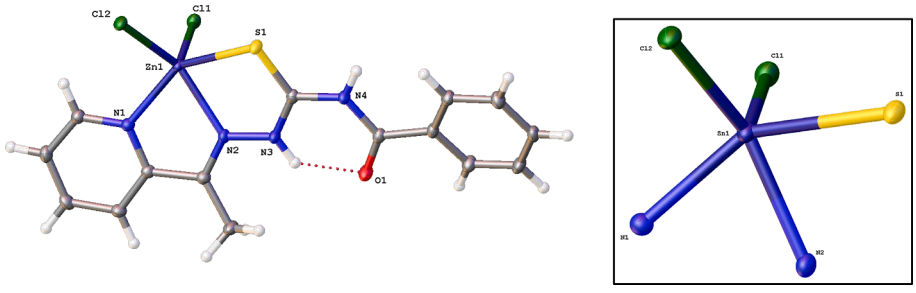


**Fig. 3.** Structure of complex **6**. Ellipsoids are drawn at 50% probability. The details of the coordination sphere and geometry is shown inset.

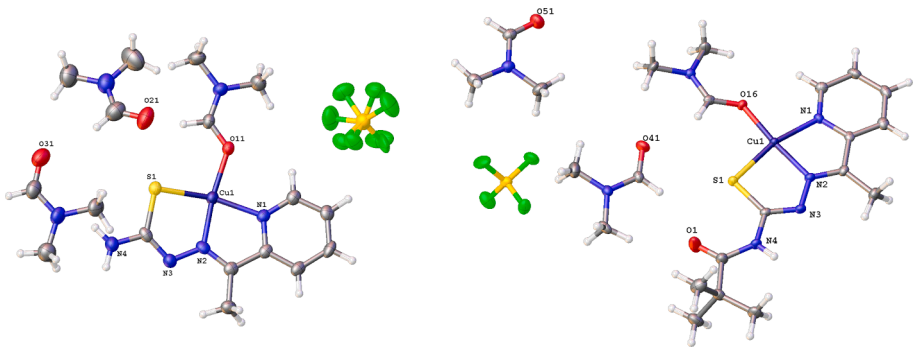


**Fig. 4.** Structures of complex **7** (left) and **8** (right). Ellipsoids are drawn at 50% probability.

**Table 8**
Selected bond lengths (Å) and bond angles (°) for complexes **11** and **12**.

| Bond lengths (Å) | **11** | **12** |
|---|---|---|
| Zn1–N4/N1 | 2.144(8) | 2.1692(13) |
| Zn1–N3/N2 | 2.152(7) | 2.1856(12) |
| Zn1–Cl1 | 2.282(2) | 2.2672(4) |
| Zn1–Cl2 | 2.290(2) | 2.2652(4) |
| Zn1–S1 | 2.453(2) | 2.4907(4) |
| Bond Angles (°) **11** | **12** | |
| N4/N1–Zn1–N3/N2 | 73.3(3) | 72.37(5) |
| N4/N1–Zn1–Cl1 | 96.4(2) | 97.76(3) |
| N3/N2–Zn1–Cl1 | 110.4(2) | 104.74(3) |
| N4/N1–Zn1–Cl2 | 93.9(2) | 96.59(3) |
| Cl1–Zn1–S1 | 101.79(8) | 105.563(14) |
| Cl2–Zn1–S1 | 98.62(8) | 95.083(14) |
| N3/N2–Zn1–Cl2 | 133.51(19) | 138.45(3) |
| Cl1–Zn1–Cl2 | 115.45(8) | 116.541(15) |
| N4/N1–Zn1–S1 | 150.79(19) | 145.69(3) |
| N3/N2–Zn1–S1 | 79.0(2) | 77.52(3) |

absorptions are assigned to the different π → π* transitions within the conjugated chromophores. The addition of the benzoyl group in **L1** appears to bathochromically shift these features, which is consistent with the added conjugation provided by this group. A very weak shoulder is apparent on the tail of the lowest energy band (337–345 nm) and this may be due to forbidden n → π* transitions that arise from the conjugated thiosemicarbazone unit.

The spectra for the Zn(II) complexes complexes **4**, **6**, **11** and **12** each show three main bands which edge into the visible region, which in turn gives the pale colour of the complexes. The two stronger features have comparable molar absorption coefficients to the free ligands and may then be attributable to perturbed ligand-based transitions. For complexes **4** and **6** these bands are subtly bathochromically shifted relative to **L1**, whereas for **11** and **12** a hypsochromic shift was noted. The lowest energy band apears around 405–410 nm for all four complexes and is about half the intensity, which is consistent with an allowed transition such as a ligand-based charge transfer.

The electronic spectra of Cu(II) complexes **1**, **2**, **7**, **8** and **9** also showed the ligand-based transitions. Cu(II) complexes are known to show LMCT transitions, and it is likely, therefore, that the strong visible band features may be S → Cu(II) CT in nature. In addition, a very weak ($\varepsilon < 200\ M^{-1}\ cm^{-1}$) and broad, longer wavelength band was observed in the region 600–650 nm which is assigned to a Cu(II)-centred d-d transition consistent with previous reports. [40,41].

For the Ni(II) complexes, the ligand-based transitions were again noted in the UV region. For complex **3**, moderately intense bands were also observed at 448 and 476 nm and are assigned to S → Ni(II) LMCT. The spectrum of complex **3** also shows a weaker shoulder feature at ~ 565 nm (which is mainly obscured by the intense CT band [42]) and a weak broad band at 816 nm. A purely octahedral Ni(II) complex is expected to show three d-d bands corresponding to $^3A_{2g}\rightarrow{}^3T_{2g}$, $^3A_{2g}\rightarrow{}^3T_{1g}$ and $^3A_{2g}\rightarrow{}^3T_{1g}(P)$ transitions and therefore we attribute these weaker features to d-d transitions. In comparison, the octahedral complex [Ni(L)$_2$] (L = S-allyl-3-[(2-pyridyl-methylene)]dithiocarbazate) published by Morsali *et. al.* [43] also shows only one d-d band at 818 nm and is thus comparable with **3**. The electronic spectra of **5** and **10**, both of which adopt an approximately square planar geometry, exhibited only one absorption band that could be identified as a likely d-d transition, at 609

**Table 9**
Selected UV–vis. absorption data for selected complexes.

| Complex | charge transfer $\lambda^{max}$ / nm (ε / $M^{-1}cm^{-1}$) | d-d transition $\lambda^{max}$ / nm (ε / $M^{-1}$ $cm^{-1}$) $d_{xy} \rightarrow d_{x2-y2}$ | $^3A_{2g}\rightarrow{}^3T_{1g}(P)$ |
|---|---|---|---|
| **1** | 421 (2600), 455 (2550) | 620(50) | – |
| **2** | 441 (7600), 457 (2300) | 634(30) | – |
| **3** | 448 (7300), 476 (1300) | – | 816 (60) |
| **5** | 382 (5500), 490 (1300) | 609(30) | – |
| **7** | 414 (6150) | 611(20) | – |
| **8** | 393 (4650) | 588(20) | – |
| **9** | 412 (4200) | 594(10) | – |
| **10** | 482 (2000) | 607(35) | – |
| **11** | 405 (5600) | – | – |
| **12** | 381 (5600) | – | – |

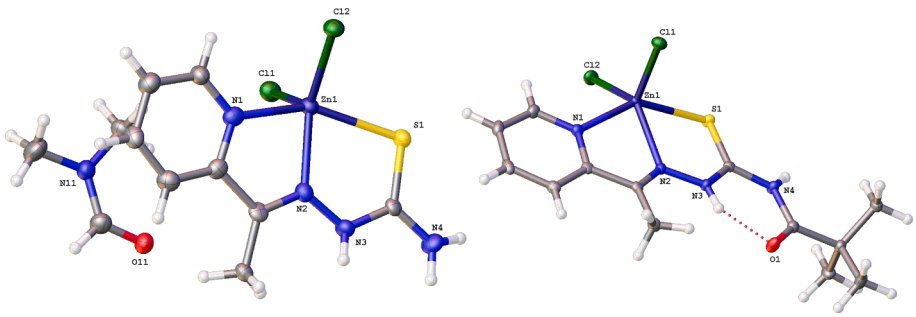


**Fig. 5.** Structures of **11** (left) and **12** (right). Ellipsoids are drawn at 50% probability.

and 607 nm, respectively. [44] This is in good agreement with the related square planar complex [Ni(L)(NCS)] (L = di-2-pyridyl ketone N (4)-phenylthiosemicarbazone), which showed ligand-based (<400 nm), LMCT (423, 449 nm) and d-d (578 nm) bands [45].

### 2.10. Magnetic susceptibility measurements

Table 10 shows the magnetic data carried out at room temperature using the Evans method, [46] which includes mass magnetic susceptibility ($\chi_{mass}$), molar magnetic susceptibility ($\chi_{molar}$) and magnetic moments ($\mu_{obs}$), for the complexes. The observed magnetic moments of the Ni(II) complexes **5** and **10** are zero confirming the diamagnetic properties of these square planar complexes. The magnetic moment for the Ni (II) complex **3** is 3.32B.M. which corresponds to two unpaired electrons consistent with an octahedral geometry. The magnetic moments of the Cu(II) complexes all fall in the range 1.76–2.15B.M. which are consistent with one unpaired electron and thus indicate that these complexes are paramagnetic and contain Cu(II). Finally, these measurements also confirmed the Zn(II) complexes were diamagnetic, as expected.

## 3. Conclusions

Two thiosemicarbazone ligands obtained from the condensation of 1-(2-pyridinyl)ethanone hydrazone and an acyl isothiocyanate, have been demonstrated to be effective ligands for Cu(II), Ni(II) and Zn(II) complexes, forming either homoleptic species or mixed ligand complexes. Through these studies the reactivity of the ligand was investigated: the pivaloyl variant (**L2**) was revealed to be sensitive to the temperature of reaction, with lower reaction temperatures required to inhibit cleavage of the pivaloyl group. The analogous benzoyl derivative (**L1**) appeared stable in all examples of its reactivity. The ligands can also act as either neutral or anionic donors depending upon the species. Eight examples of the coordination complexes were successfully characterised using single crystal X-ray diffraction. In all cases the ligands coordinate in a tridentate manner via a $N_2S$ donor set. These structural studies confirmed the nature of coordination and included examples of anionic and neutral ligand forms. A variation in complex geometries were noted, including both 5-coordinate square pyramidal and 4-coordinate square planar structures for Cu(II), 4-coordinate square planar for Ni(II) and 5-coordinate, approximately trigonal bipyramidal to spherical square pyramidal, for Zn(II). Given the importance of the biological aspects of thiosemicarbazones outlined earlier, further studies will investigate these, and other related complexes, and investigate their bioactivity and potential applications.

## 4. Experimental

### 4.1. Instrumentation

All reagents and solvents were purchased from commercial suppliers and used without further purification. Single crystals X-ray data were carried out by university of Southampton, UK national crystallography service. The $^{1}H$ NMR and $^{13}C$ spectra were recorded in DMSO-*d*6 and $CDCl_3$ on a Bruker-250-400 MHz spectrophotometer using tetramethylsilane as an internal reference. Infrared spectra were recorded in the range 400-4000 $cm^{-1}$ on a Jasco 660 FT-IR spectrophotometer. Electrospray (ES) and high-resolution (HR) mass spectra were measured on a Waters LCT Premier XE (oa- TOF) mass spectrometer. Magnetic susceptibility measurements of the Cu(II) and Ni(II) complexes were carried out in DMSO-$d_6$ for 0.020 mol.$L^{-1}$ solutions at room temperature (24 °C) by employing the Evans method.[40] The Evans method uses difference in the NMR chemical shift in a solvent caused by the presence of a paramagnetic species and the effective magnetic moments were calculated using the relation $\mu_{eff} = 2.828\ (\chi_{m}.T)^{1/2}$B.M., where $\chi_m$ is the molar susceptibility. Electronic spectra were recorded on a Shimadzu UV1601 spectrophotometer in DMF from 230 to 1100 nm. Elemental analyses were carried out by the London Metropolitan University.

**Table 10**
Magnetic data for selected complexes.

| Complex | $\chi_{mass} \times 10^{-6}$ | $\chi_{molar} \times 10^{-6}$ | $\mu_{obs}$ (B.M.) |
|---|---|---|---|
| **1** | 2.986 | 1551.06 | 1.92 |
| **2** | 1.979 | 1700.77 | 2.01 |
| **3** | 5.462 | 4666.34 | 3.32 |
| **7** | 3.412 | 1421.85 | 1.84 |
| **8** | 2.584 | 1291.84 | 1.76 |
| **9** | 2.466 | 1957.60 | 2.15 |

## 5. X-ray crystallography

Suitable crystals of **1, 5, 6, 7, 8, 10, 11, 12** were selected and data collected following a standard method. [47] In each case, a crystal was selected and mounted on a MITIGEN holder in oil on a Rigaku FRE+ (Mo) diffractometer equipped with an AFC12 goniometer and HG Saturn 724 + detector with either VHF (1, 6, 10, 11, 12) or HF (5, 7, 8) Varimax confocal mirrors. The crystals were kept at a steady T = 100(2) K during data collection using an Oxford Cryosystems low-temperature device. The structures were solved with the ShelXT [48] structure solution program using the Intrinsic Phasing solution method and by using Olex2 [49] as the graphical interface. The models were refined with version 2018/3 of ShelXL [50] using Least Squares minimisation. CCDC2179007-2179014 contains supplementary X-ray crystallographic data for **1, 5, 6, 7, 8, 10, 11, 12** respectively. This data can be obtained free of charge via https://www.ccdc.cam.ac.uk/conts/retrieving.html, or from the Cambridge Crystallographic Data Centre, Union Road, Cambridge, CB2 1EZ; fax(+44) 1223–336-033 or email: deposit@ccdc.cam.ac.uk.

***CAUTION*:** Perchlorate compounds of metal ions are potentially explosive especially in presence of organic ligands. Given the reactions here that combine hydrazones with perchlorates, only a very small amount of material should be prepared and handled with great care.

### 5.1. Synthesis of L1

**L1** was synthesized via a modified method described before. [51] The starting material 1-(2-pyridinyl)ethanone hydrazine [52] (1.35 g, 10 mmol) was dissolved in acetonitrile (20 $cm^3$) and benzoyl isothiocyanate (1.63 g, 10 mmol) in acetonitrile (15 $cm^3$) were heated at reflux for 3 h. A yellow precipitate was formed, washed with acetonitrile (10 $cm^3$) and recrystallized from acetonitrile to yield yellow crystals, which were dried under vacuum. Yield (1.20 g, 90 %); m.p = 174-176°C; EI-MS (*m/z*) (%): 298.09 [M] (80 %); Mass: 298.0884, Calc Mass: 298.0888; Selected FT-IR ($cm^{-1}$): ν(N—H) 3391, ν(C═O) 1663, ν(C═S) 1332; UV–vis., $\lambda^{max}$ (nm) (ε, $M^{-1}$ $cm^{-1}$): 287 (14500), 345 (10800). $^{1}H$ NMR (400 MHz, DMSO-$d_6$), δ (ppm): 13.88 (1H, s, N*H*), 11.88 (1H, s, N*H*), 8.66 (1H, d, $J_{HH}$ = 2.5 Hz), 8.18 (1H, d, $J_{HH}$ = 5 Hz), 8.01 (2H, d, $J_{HH}$ = 5 Hz), 7.93 (1H, app. t, $J_{HH}$ = 7.5 Hz), 7.68 (1H, app. t, $J_{HH}$ = 7.5 Hz), 7.55 (2H, app. t, $J_{HH}$ = 5 Hz), 7.49 (1H, app. t, $J_{HH}$ = 5 Hz), 2.48 (3H, s, C$H_3$); $^{13}C\{^{1}H\}$ NMR (125 MHz, DMSO-$d_6$), δ (ppm): 177.8 (*C*S), 168.7 (*C*O), 156.5, 154.2, 148.8, 136.8, 133.2, 131.8, 128.8, 128.5, 124.7, 120.9, 12.4 (*C*$H_3$).

### 5.2. Synthesis of L2

To a suspension of potassium thiocyanate (0.97 g, 10 mmol) in acetonitrile (10 $cm^3$) was added dropwise, a solution of trimethyl acetyl chloride (1.2 g, 10 mmol) in acetonitrile (15 $cm^3$). The reaction mixture was heated at reflux for 3 h. A yellow solution formed together with a white precipitate (KCl) which was removed by filtration. The resultant yellow filtrate solution was then added to a solution of 1-(2-pyridinyl) ethanone hydrazone (1.35 g, 10 mmol) in acetonitrile (5 $cm^3$) and the

reaction mixture was stirred at room temperature for 24 h. A light yellow precipitate was formed, collected by filtration and washed with acetonitrile:ethanol (1:1, 10 $cm^3$) and purified by recrystallization from ethanol to obtain light yellow crystals. Yield (1.00 g, 81 %); m.p = 141-142ºC, ES-MS (*m/z*)(%): 278.12 [M] (70 %); Mass: 278.1206, Calc. Mass: 278.1201. Selected FT-IR ($cm^{-1}$): ν(N—H) 3298, ν(C═O) 1672, ν (C═S) 1371; UV–vis., $\lambda^{max}$ (nm), (ε, $M^{-1}$ $cm^{-1}$): 270 (21800), 337 (23350). $^1$H NMR (400 MHz, DMSO-$d_6$), δ (ppm): 13.79 (1H, s, N*H*), 10.91 (1H, s, N*H*), 8.64 (1H, d, $J_{HH}$ = 2.5 Hz), 8.14 (1H, d, $J_{HH}$ = 2.5 Hz), 7.92 (1H, app. t, $J_{HH}$ = 7.5 Hz), 7.48 (1H, app. t, $J_{HH}$ = 5 Hz), 2.42 (3H, s, C*H*$_3$), 1.27 (9H, s, C*H*$_3$); $^{13}$C{$^1$H} NMR (100 MHz, DMSO-$d_6$), δ (ppm): 180.8 (*C*S), 178.1 (*C*O), 156.2, 154.1, 148.8, 136.8, 124.7, 120.9, 39.9, 26.2 (*C*H$_3$), 12.5 (*C*H$_3$).

### 5.3. Synthesis of complexes (1 – 12)

***CAUTION*:** Perchlorate compounds of metal ions are potentially explosive especially in the presence of organic ligands. Only a small amount of material should be prepared and handled with care.

### 5.4. Synthesis of $[(L1^-)Cu^{II}(MeCN)(H_2O)]ClO_4$ (1)

A solution of $Cu(ClO_4)_2{\cdot}6H_2O$ (0.37 g, 0.0010 mol) in water (5 $cm^3$) was added to a solution of **L1** (0.3 g, 0.0010 mol) in DMF (5 $cm^3$). The mixture was allowed to stir for 4 h at room temperature. The colourless solution turned to dark green with a precipitate. At this time, the green precipitate formed was filtered, washed with DMF (5 $cm^3$) to remove unreacted **L1** and dried in rotary evaporator. Green crystals of **1** were grown at room temperature from acetonitrile by the diffusion of diethyl ether vapour. Yield: (0.20 g, 65 %); green crystals; ESI-MS (*m/z*)(%): 417.98 [M−H] (100 %); Selected FT-IR ($cm^{-1}$): ν(N—H) 3429, ν(C═O) 1660, δ(N—H) 1597, ν(C═N) 1476, ν(C═S) 1263, ν(Cl-O) 1092, 621; UV–vis., $\lambda^{max}$ (nm) (ε, $M^{-1}$ $cm^{-1}$): 267 (50000), 303 (44150), 421 (2600), 455(2550), 620(47); Anal. Calcd. for $C_{17}H_{18}ClCuN_5O_6S$**:** C, 39.31; H, 3.49; N,13.48 %. Found: C, 39.15; H, 3.49; N, 13.47 %.

### 5.5. Synthesis of $[Cu(L1)_2](ClO_4)_2$ (2)

A solution of $Cu(ClO_4)_2{\cdot}6H_2O$ (0.186 g, 0.0005 mol) in $H_2O$ (5 $cm^3$) was added to a solution of **L1** (0.3 g, 0.0010 mol) in DMF (5 $cm^3$). The mixture was allowed to stir for 6 h at room temperature. The colourless solution turned to light green with a precipitate. At this time, the light green precipitate formed was filtered, washed with DMF (5 $cm^3$) to remove unreacted **L1** and dried in rotary evaporator. Yield (0.21 g, 65 %); green powder; ESI-MS (*m/z*)(%): ESI-MS (*m/z*)(%): 657.15 [M−H] (100 %); Mass: 657.1480, calc. Mass: 657.1471; Selected FT-IR ($cm^{-1}$): ν(N—H) 3410, ν(C═O) 1662, ν(C═S) 1258; ν(Cl-O) 1096, 621; UV–vis., $\lambda^{max}$ (nm) (ε, $M^{-1}$ $cm^{-1}$): 274 (21300), 299 (23200), 441 (7600), 457 (2300), 634 (25); Anal. Calcd. for $C_{30}H_{26}Cl_2CuN_8O_{10}S_2$: C, 42.04; H, 3.06; N,13.07 %. Found: C, 42.02; H, 3.20; N, 13.27 %.

### 5.6. Synthesis of $[Ni(L1)_2](ClO_4)_2$ (3)

A solution of $Ni(ClO_4)_2{\cdot}6H_2O$ (0.183 g, 0.0005 mol) in methanol (5 $cm^3$) and a solution of **L1** (0.3 g, 0.0010 mol) in $CHCl_3$ (10 $cm^3$) was stirred at 50 °C for 7 h. The brown coloured solution formed and the resultant brown precipitate was filtered, washed with $CHCl_3$ (2 × 20 $cm^3$) to remove the unreacted ligand and dried on a rotary evaporator. Yield (0.26 g, 87 %); brown powder; ESI-MS (*m/z*)(%): 653.13 [M + ] (100 %); 653.1057 Calc. Mass: 653.1052; Selected FT-IR ($cm^{-1}$): ν (N—H) 3350, ν(C═O) 1660, δ(N—H) 1601, δ(N—H) 1538, ν(C═N) 1472, ν(C═S) 1252, ν(Cl-O) 1093, 622; UV–vis., $\lambda^{max}$ (nm) (ε, $M^{-1}$ $cm^{-1}$): 267 (15150), 296 (19500), 448 (7300), 476 (1300), 816 (63). Anal. Calcd. for $C_{30}H_{28}Cl_2N_8NiO_{10}S_2$: C, 42.18; H, 3.30; N,13.12 %. Found: C, 42.25; H, 3.24; N, 13.13 %.

### 5.7. Synthesis of $[Zn(L1)_2](ClO_4)_2$ (4)

A methanolic solution (5 $cm^3$) of $Zn(ClO_4)_2{\cdot}6H_2O$ (0.186 g, 0.0005 mol) was added drop wise to a solution of **L1** (0.3 g, 0.0010 mol) in $CHCl_3$ (5 $cm^3$). The mixture was stirred for 8 h at room temperature. The resultant white-creamy precipitate was filtered, washed with $CHCl_3$ (2 × 10 $cm^3$), and methanol (10 $cm^3$) to remove the unreacted ligand, and dried on a rotary evaporator. Yield (0.23 g, 77 %); white-creamy powder; ESI-MS (*m/z*)(%): 659.12 [M + ] (100 %); Mass: 659.0995, Calc. Mass: 659.0990; Selected FT-IR ($cm^{-1}$): ν(N—H) 3366, ν(C═O) 1663, ν (C═S) 1250, ν(Cl-O) 1096, 619; UV–vis., $\lambda^{max}$ (nm) (ε, $M^{-1}$ $cm^{-1}$): 290 (89400), 360 (38000), 409 (32800); $^1$H NMR (400 MHz, DMSO-$d_6$), δ (ppm): 13.40 (2H, s, N*H*), 11.53 (2H, s, N*H*), 8.39 (2H, m), 8.08 (2H, d, $J_{HH}$ = 5 Hz), 8.02 (2H, m), 7.83 (4H, d, $J_{HH}$ = 5 Hz), 7.54 (4H, m), 7.43 (4H, m), 2.39 (6H, s, C*H*$_3$); $^{13}$C{$^1$H} NMR (100 MHz, DMSO-$d_6$), δ(ppm): 177.6 (*C*S), 167.7 (*C*O), 155.8, 150.5, 148.1, 140.9, 133.3, 132.9, 128.9, 128.7, 124.7, 122.0, 14.1 (*C*H$_3$). Anal. Calcd. for $C_{30}H_{28}Cl_2N_8O_{10}S_2Zn$: C, 41.85; H, 3.28; N,13.01 %. Found: C, 41.76; H, 3.27; N, 13.14 %.

### 5.8. Synthesis of $[NiCl(L1^-)]$ (5)

A solution of $NiCl_2{\cdot}6H_2O$ (0.24 g, 0.0010 mol) in methanol (5 $cm^3$) and a solution of **L1** (0.3 g, 0.0010 mol) in $CHCl_3$ (10 $cm^3$) were stirred at 40 °C for 4 h. The colourless solution turned to brown. The resultant brown precipitate was filtered, washed with $CHCl_3$ (2 × 20 $cm^3$) and methanol (10 $cm^3$) to remove the unreacted ligand and Ni salt and dried on a rotary evaporator. Yield (0.21 g, 70 %); red crystals; ESI-MS (*m/z*) (%): 389.01 [M + ] (100 %); 388.9760 Calc. Mass: 388.9774; Selected FT-IR ($cm^{-1}$): ν(N—H) 3310, ν(C═O) 1664, ν(C═S) 1263; UV–vis., $\lambda^{max}$ (nm) (ε, $M^{-1}$ $cm^{-1}$): 281 (10400), 300 (12200), 382 (5500), 490 (1300), 609 (29). Anal. Calcd. for $C_{15}H_{13}ClN_4NiOS$: C, 46.02; H, 3.35; N,14.31 %. Found: C, 46.24; H, 3.07; N, 14.29 %.

### 5.9. Synthesis of $[ZnCl_2(L1)]$ (6)

An ethanolic solution (5 $cm^3$) of $ZnCl_2$ (0.14 g, 0.0010 mol) was added drop wise to a solution of **L1** (0.3 g, 0.0010 mol) in $CHCl_3$ (5 $cm^3$). The mixture was stirred at 40° C for 4 h. The resultant white-creamy precipitate was filtered, washed with $CHCl_3$ (10 $cm^3$) and ethanol (5 $cm^3$) and dried on a rotary evaporator. Yield: (0.2 g, 67 %); light yellow crystals; ESI-MS (*m/z*)(%): 463.95 [M + MeOH] (100 %); Selected FT-IR ($cm^{-1}$): ν(N—H) 3279, ν(C═O) 1663, ν(C═S) 1270; UV–vis., $\lambda^{max}$ (nm) (ε, $M^{-1}$ $cm^{-1}$): 289 (11400), 355 (5100), 409 (3250); $^1$H NMR (400 MHz, DMSO-$d_6$), δ (ppm): 13.87 (1H, s, N*H*), 11.74 (1H, s, N*H*), 8.64 (1H, m), 8.14 (1H, d, $J_{HH}$ = 5 Hz), 8.03 (1H, m), 7.93 (2H, d, $J_{HH}$ = 5 Hz), 7.62 (2H, m), 7.51 (2H, app. t, $J_{HH}$ = 5 Hz), 2.47 (3H, s, C*H*$_3$); $^{13}$C {$^1$H} NMR (100 MHz, DMSO-$d_6$), δ (ppm): 177.4 (*C*S), 168.3 (*C*O), 155.6, 148.2, 137.6, 133.3, 132.4,128.9, 128.7, 125.9, 123.1, 13.5 (*C*H$_3$). Anal. Calcd. for $C_{15}H_{14}Cl_2N_4OSZn$: C, 41.45; H, 3.25; N,12.89 %. Found: C, 41.29; H, 3.27; N, 12.93 %.

### 5.10. Synthesis of $[Cu(DMF)(L2'^-)]BF_4$ (7)

A solution of $Cu(BF_4)_2{\cdot}6H_2O$ (0.26 g, 0.00108 mol) in methanol (5 $cm^3$) was added to a solution of **L2** (0.3 g, 0.00108 mol) in $CHCl_3$ (5 $cm^3$). The mixture was allowed to stir for 10 h at room temperature. The colourless solution turned to dark green with a precipitate. The green precipitate formed was filtered, washed with $CHCl_3$ (10 $cm^3$) and dried on a rotary evaporator. Green crystals of the product were grown at room temperature from dimethylformamide by the diffusion of diethyl ether vapour. Yield: (0.22 g, 74 %); dark green crystals; ESI-MS (*m/z*) (%): 353.31 [M + $Na^+$,$H^+$] (100 %); Selected FT-IR ($cm^{-1}$): ν(N—H) 3333, 1710 (C═O), ν(C═S) 1310; UV–vis., $\lambda^{max}$ (nm) (ε, $M^{-1}$ $cm^{-1}$): 297 (12800), 414 (6150), 611 (19). Anal. Calcd. for $C_{11}H_{16}BCuF_4N_5OS$: C, 31.71; H, 3.87; N,16.81 %. Found: C, 31.82; H, 3.78; N, 16.72 %.

### 5.11. Synthesis of [Cu(L2$^-$)(DMF)]$BF_4$ (8)

A solution of $Cu(BF_4)_2{\cdot}6H_2O$ (0.26 g, 0.00108 mol) in DMF (5 $cm^3$) was added to a solution of **L2** (0.3 g, 0.00108 mol) in DMF (5 $cm^3$). The mixture was cooled in an ice bath and allowed to stir for 10 h. The colourless solution turned to dark green with a precipitate. The green precipitate was filtered, washed with DMF (5 $cm^3$) and dried on a rotary evaporator. Green crystals of [Cu(L2$^-$)(DMF)]$BF_4$ were grown at room temperature from dimethylformamide by the diffusion of diethyl ether vapour. Yield: (0.19 g, 64 %); green crystals; ESI-MS (*m/z*)(%): 413.11 (100 %); Mass: 413.0947, Calc. Mass: 413.0947; Selected FT-IR ($cm^{-1}$): ν(N—H) 3335, ν(C═O) 1707, ν(C═O) 1670, ν(C═S) 1322; UV–vis., $\lambda^{max}$ (nm), (ε, $M^{-1}$ $cm^{-1}$): 287 (13500), 393 (4650), 588 (23). Anal. Calcd. for $C_{16}H_{24}BCuF_4N_5O_2S$: C, 38.37; H, 4.83; N,13.98 %. Found: C, 38.26; H, 4.89; N, 13.86 %.

### 5.12. Synthesis of [Cu(L2)$_2$](BF$_4$)$_2$ (9)

A solution of $Cu(BF_4)_2{\cdot}6H_2O$ (0.13 g, 0.00054 mol) in DMF (5 $cm^3$) was added to a solution of **L2** (0.3 g, 0.00108 mol) in DMF (5 $cm^3$). The mixture was cooled in an ice bath and allowed to stir for 10 h. The colourless solution turned to dark green with a precipitate. The green precipitate formed was filtered, washed with DMF (5 $cm^3$) and dried on a rotary evaporator. Green crystals of **9** were grown at room temperature from dimethylformamide by the diffusion of diethyl ether vapour. Yield: (0.2 g, 68 %); green crystals; ESI-MS (*m/z*)(%): 618.21 [M + ] (100 %); Mass: 618.1889, Calc. Mass: 618.1897; Selected FT-IR ($cm^{-1}$): ν(N—H) 3329, ν(C═O) 1669, ν(C═S) 1330; UV–vis., $\lambda^{max}$ (nm) (ε, $M^{-1}$ $cm^{-1}$): 278 (67500), 412 (4200), 594 (11); Anal. Calcd. for $C_{26}H_{34}B_2CuF_8N_8O_2S_2$: C, 39.44; H, 4.33; N,14.15 %. Found: C, 39.41; H, 4.67; N, 14.14 %.

### 5.13. Synthesis of [NiCl(L2$^-$)] (10)

A solution of $NiCl_2{\cdot}6H_2O$ (0.26 g, 0.00108 mol) in methanol (5 $cm^3$) and a solution of **L2** (0.3 g, 0.00108 mol) in $CHCl_3$ (10 $cm^3$) were stirred for 24 h at room temperature. The colourless solution turned to brown. The resultant brown precipitate was filtered, washed with diethyl ether (2 × 20 $cm^3$) and dried on a rotary evaporator. Orange crystals of **10** were grown at room temperature by the diffusion of diethyl ether vapour into an acetonitrile solution. Yield: (2.4 g, 80 %); orange crystals; ESI-MS (*m/z*)(%): 393.00 [M + Na] (80 %); Selected FT-IR ($cm^{-1}$): ν (N—H) 3314, ν(C═O) 1671, ν(C═S) 1337; UV–vis., $\lambda^{max}$ (nm) (ε, $M^{-1}$ $cm^{-1}$): 266 (19800), 303 (19500), 381 (12300), 482 (2000), 607 (35). Anal. Calcd. for $C_{13}H_{17}ClN_4NiOS$: C, 42.03; H, 4.61; N,15.08 %. Found: C, 41.95; H, 4.57; N, 14.78 %.

### 5.14. Synthesis of [Zn(L2′)Cl$_2$] (11)

An ethanolic solution (10 $cm^3$) of $ZnCl_2$ (0.147 g, 0.00108 mol) was added drop wise to a solution of **L2** (0.3 g, 0.00108 mol) in $CHCl_3$(5 $cm^3$). The mixture was heated at 40° C for 5 h. The white-creamy precipitate formed was filtered, washed with $CHCl_3$ (5 $cm^3$), and ethanol (5 $cm^3$) and dried on a rotary evaporator. Yellow crystals of **11** were grown at room temperature by the diffusion of diethyl ether vapour into a DMF solution. Yield: (0.22 g, 75 %); Yellow crystals; ESI-MS (*m/z*)(%): 328.90 [M + H] (100 %); Selected FT-IR ($cm^{-1}$): ν (N—H) 3170, ν(C═S) 1321; UV–vis., $\lambda^{max}$ (nm) (ε, $M^{-1}$ $cm^{-1}$): 269 (17500), 332 (14800), 405 (5600); $^1$H NMR (400 MHz, DMSO-$d_6$), δ (ppm): 10.91 (1H, s, N*H*), 8.66 (1H, d, $J_{HH}$ = 5 Hz), 8.16 (1H, d, $J_{HH}$ = 5 Hz), 8.05 (1H, app. t, $J_{HH}$ = 5 Hz), 7.60 (1H, app. t, $J_{HH}$ = 5 Hz), 4.34 (2H, s, N$H_2$), 2.46 (3H, s, C$H_3$); $^{13}$C{$^1$H} NMR (101 MHz, DMSO-$d_6$), δ (ppm): 178.5 (*CS*), 155.8, 149.0, 148.6, 137.7, 126.6, 123.8, 13.2 (C$H_3$) ppm. Anal. Calcd. for $C_8H_{10}Cl_2N_4SZn$: C, 29.07; H, 3.05; N, 16.95 %. Found: C, 29.04; H, 2.95; N, 16.81 %.

### 5.15. Synthesis of [Zn(L2)Cl$_2$] (12)

A DMF solution (3 $cm^3$) of $ZnCl_2$ (0.15 g, 0.00108 mol) was added drop wise to a solution of L2 (0.3 g, 0.00108 mol) in DMF (3 $cm^3$). The mixture was stirred at 0° C for 5 h. The resultant white-creamy precipitate formed was filtered, washed with DMF (2 $cm^3$) and dried on a rotary evaporator. Yield: (0.18 g, 63 %); white-creamy powder; ESI-MS (*m/z*)(%): 411.93 [M + H] (70 %); Mass: 412.1566, Calc. Mass: 412.1575; Selected FT-IR ($cm^{-1}$): ν (N—H) 3167, ν (C═O) 1670, ν (C═S) 1340; UV–vis., $\lambda^{max}$ (nm) (ε, $M^{-1}$ $cm^{-1}$): 266 (12400), 321 (9300), 381 (5600); $^1$H NMR (400 MHz, DMSO-$d_6$), δ (ppm): 14.06 (1H, s, N*H*), 11.28 (1H, s, N*H*), 8.66 (1H, d, $J_{HH}$ = *2*.5 Hz), 8.15 (1H, d, $J_{HH}$ = 5 Hz), 8.04 (1H, app. t, $J_{HH}$ = 7.5 Hz), 7.59 (1H, app. t, $J_{HH}$ = *7*.5 Hz), 2.46 (3H, s, C*H*$_3$), 1.25 (9H, s, C*H*$_3$); $^{13}$C{$^1$H} NMR (100 MHz, DMSO-$d_6$), δ (ppm): 178.0 (*CS*), 171.3 (*CO*), 159.2, 155.8, 148.6, 138.1, 128.0, 120.6, 39.6, 26.1 (*CH*$_3$), 13.5 (*CH*$_3$). Anal. Calcd. for $C_{13}H_{18}Cl_2N_4OSZn$: C, 37.66; H, 4.38; N, 13.51 %. Found: C, 38.05; H, 4.69; N, 13.41 %.

## CRediT authorship contribution statement

**Ali A.A. Al-Riyahee:** Investigation, Validation, Writing – original draft. **Peter N. Horton:** Investigation, Validation, Writing – review & editing. **Simon J. Coles:** Writing – review & editing. **Angelo J. Amoroso:** Conceptualization, Methodology, Supervision, Writing – review & editing. **Simon J. A. Pope:** Supervision, Writing – original draft, Writing – review & editing.

## Declaration of Competing Interest

The authors declare that they have no known competing financial interests or personal relationships that could have appeared to influence the work reported in this paper.

## Data availability

Data will be made available on request.

## Appendix A. Supplementary data

Supplementary data to this article can be found online at https://doi.org/10.1016/j.poly.2022.116079.

## References

[1] For example, N. Balakrishnan, J. Haribabu, R.E. Malekshah, S. Swaminathan, C. Balachandran, N. Bhuvanesh, S. Aoki, R. Karvembu, Inorg, Chim. Acta 534 (2022) 120805; S.A. Elsayed, H.E. Badr, A. di Biase, A.M. El-Hendawy, J. Inorg. Biochem. 223 (2021) 111549; N. Gomez, D. Santos, R. Vazquez, L. Suescun, A. Mombru, M. Vermeulen, L. Finkielsztein, C. Shayo, A. Moglioni, D. Gambino, C. Davio, ChemMedChem 6 (2011) 1485; L.A. Al-Doori, A.A. Irzoqi, H.M. Jirjes, A.H. Al-Obaidi, M.A. Alheety, Inorg. Chem. Commun. 140 (2022) 109454; S. Eglence-Bakir, J. Mol. Struct. 1246 (2021) 131121.

[2] E. M. Jouad, G. Larcher, M. Allain, A. Riou, G. M. Bouet, M. A. Khan, X. D. Thanh, J. Inorg. Biochem. 86 (2001) 565; S. A. Patil, V. H. Naik, A. D. Kulkarni, P. S. Badami, Spectrochim. Acta A 75 (2010) 347.

[3] H. Beraldo, Quim. Nova 27 (2004) 461; D. Kovala-Demertzi, J. R. Miller, N. Kourkoumelis, S. K. Hadjikakou, M. A. Demertzis, Polyhedron 18 (1999) 1005; R. W. Byrnes, M. Mohan, W. E. Antholine, R. X. Xu, D. H. Petering, Biochemistry 29 (1990) 7046.

[4] D. Hamre, J. Bernstein, R. Donovick, Proc. Soc. Exp. Biol. Med. 73 (1950) 275; C. Shipman, S. H. Smith, J. C. Drach, D. L. Klayman, Antiviral Res. 6 (1986) 197; P. Tarasconi, S. Capacchi, G. Pelosi, M. Cornia, R. Albertini, A. Bonati, P. P. Dall'Aglio, P. Lunghi, S. Pinelli, Bioorg. Med. Chem. 8 (2000) 157.

[5] F.R. Pavan, P.I. da, S. Maia, S.R.A. Leite, V.M. Deflon, A.A. Batista, D.N. Sato, S. G. Franzblau, C.Q.F. Leite, Eur. J. Med. Chem. 45 (2010) 1898.

[6] R. H. Dodd, C. Ouannès, M. Robert-Gèro and P. Potier, J. Med. Chem. 32 (1989) 1272; S. Chandra and L. K. Gupta, Spectrochim. Acta - Part A 62 (2005) 1089; M. Belicchi, G. Gasparri, E. Leporati, G. Pelosi, R. Rossi, P. Tarasconi, R. Albertini, A. Bonati, P. Lunghi and S. Pinelli, J. Inorg. Biochem. 70 (1998) 145; M. B. Ferrari, S. Capacchi, G. Reffo, G. Pelosi, P. Tarasconi, R. Albertini, S. Pinelli and P. Lunghi, J. Inorg. Biochem. 81 (2000) 89.

[7] R.B. de Oliveira, E.M. de Souza-Fagundes, R.P.P. Soares, A.A. Andrade, A.U. Krettli, C.L. Zani, Eur. J. Med. Chem. 43 (2008) 1983.
[8] A. Mrozek-Wilczkiewicz, K. Malarz, M. Rejmund, J. Polanski, R. Musiol, Eur. J. Med. Chem. 171 (2019) 180.
[9] M. Serda, A. Mrozek-Wilczkiewicz, J. Jampilek, M. Pesko, K. Kralova, M. Vejsova, R. Musiol, A. Ratuszna, J. Polanski, Molecules 17 (2012) 13483.
[10] W. Cheng, T. Xiao, W. Qian, T. Lu, T. Zhang, X. Tang, Nat. Prod. Res. 35 (2021) 3801.
[11] F. Degola, C. Morcia, F. Bisceglie, F. Mussi, G. Tumino, R. Ghizzoni, G. Pelosi, V. Terzi, A. Buschini, F.M. Restivo, T. Lodi, Int. J. Food Microbiol. 200 (2015) 104.
[12] N.P. Prajapati, H.D. Patel, Synth. Commun. 49 (2019) 2767; F. Basuli, M. Ruf, C.G. Pierpont, S. Bhattacharya, Inorg. Chem. 37 (1998) 6113.
[13] G. Pelosi, Open Crystallogr. J. 3 (2010) 16.
[14] T. Rosu, A. Gulea, A. Nicolae, R. Georgescu, Molecules 12 (2007) 782.
[15] D. Rogolino, A. Gatti, M. Carcelli, G. Pelosi, F. Bisceglie, F.M. Restivo, F. Degola, A. Buschini, S. Montalbano, D. Feretti, C. Zani, Sci. Rep. 7 (2017) 11214.
[16] N.P. Prajapati, H.D. Patel, Synth. Commun. 49 (2019) 2767; F. Basuli, M. Ruf, C.G. Pierpont, S. Bhattacharya, Inorg. Chem. 37 (1998) 6113.
[17] D.L. Klayman, J.P. Scovill, J.F. Bartosevich, C.J. Mason, J. Med. Chem. 22 (1979) 1367.
[18] J.P. Scovill, D.L. Klayman, C.F. Franchino, J. Med. Chem. 25 (1982) 1261.
[19] A. I. Matesanz, J. M. Perez, P. Navarro, J. M. Moreno, E. Colacio, P. Souza, J. Inorg. Biochem. 76 (1999) 29; P.K. Suganthy, R.N. Prabhu, V.S. Sridevi, Inorg. Chem. Commun. 44 (2014) 67.
[20] E. Labisbal, A. Sousa, A. Castineiras, J.A. Garcia-Vazquez, J. Romero, D.X. West, Polyhedron 19 (2000) 1255.
[21] S.G. Teoh, S.H. Ang, H.K. Fun, C.W. Ong, J. Organomet. Chem. 580 (1999) 17.
[22] A. Castiñeiras, I. Garcia, E. Bermejo, D. X. West, Polyhedron 19 (2000) 1873; I. Garcıa, E. Bermejo, A. K. El Sawaf, A. Castineiras, D.X. West, Polyhedron 21 (2002) 729.
[23] P.P. Netalkar, S.P. Netalkar, V.K. Revankar, Polyhedron 100 (2015) 215.
[24] D.K. Demertzi, P.N. Yadav, M.A. Demertzis, M. Coluccia, J. Inorg. Biochem. 78 (2000) 347.
[25] T.A. Yousef, G.M. Abu El-Reach, R.M. El Morshedy, J. Mol. Structure 1045 (2013) 145; T.A. Yousef, G.M. Abu El-Reash, O.A. El-Gammal, R.A. Bedier, J. Mol. Structure 1029 (2012) 149.
[26] R.B. Singh, B.S. Garg, R.P. Singh, Talanta 25 (1978) 619.
[27] A.R. Cowley, J.R. Dilworth, P.S. Donnelly, J.M. White, Inorg. Chem. 45 (2006) 496.
[28] B.M. Paterson, P.S. Donnelly, Chem. Soc. Rev. 40 (2011) 3005.
[29] Y. Fujibayashi, H. Taniuchi, Y. Yonekura, H. Ohtani, J. Konishi, A. Yokoyama, J. Nucl. Med. 38 (1997) 1155; A.L. Vavere, J.S. Lewis, Dalton Trans. 43 (2007) 4893; J.S. Lewis, R. laforest, F. Dehdashti, P.W. Grigsby, M.J. Welch, B.A. Siegel, J. Nucl. Med. 49 (2008) 1177.
[30] M. Columbie, S. Gouard, M. Frindel, A. Vidal, M. Cherel, F. Kraeber-Bodere, C. Rousseau, M. Bourgeois, Front. Med. 2 (2015) 00058.
[31] A.A.A. Al-Riyahee, P.N. Horton, S.J. Coles, C. Berry, P.D. Horrocks, S.J.A. Pope, A. J. Amoroso, Dalton Trans. 51 (2022) 3531.
[32] K.A. Ketcham, J.K. Swearingen, A. Castineiras, I. Garcia, E. Bermejo, D.X. West, Polyhedron 20 (2001) 3265.
[33] R. Gil-García, R. Fraile, B. Donnadieu, G. Madariaga, V. Januskaitis, J. Rovira, L. González, J. Borrás, F.J. Arnáiz, J. García-Tojal, New J. Chem. 37 (2013) 3568.
[34] A. Murugkar, R. Bendre, S. Padhye, Ind. J. Chem. 38A (1999) 981.
[35] M. Llunell, D. Casanova, J. Gierera, P. Alemany, S. Alvarez, SHAPE, Continuous Shape Measures Calculation, version 2.0; Universitat de Barcelona: Barcelona, Spain, 2010.
[36] N.C. Kasuga, K. Sekino, M. Ishikawa, A. Honda, M. Yokoyama, S. Nakano, N. Shimada, C. Koumo, K.J. Nomiya, Inorg. Biochem. 96 (2003) 298.
[37] P.J. Jansson, P.C. Sharpe, P.V. Bernhardt, D.R.J. Richardson, Med. Chem. 53 (2010) 5759.
[38] M.B. Ferrari, F. Bisceglie, G. Pelosi, P. Tarasconi, R. Albertini, S. Pinelli, J. Inorg. Biochem. 87 (2001) 137.
[39] C.R. Kowol, R. Trondl, V.B. Arion, M.A. Jakupec, I. Lichtscheidl, B.K. Keppler, Dalton Trans. 39 (2010) 704.
[40] D.X. West, J.S. Ives, J. Krejci, M.M. Salberg, T.L. Zumbahlen, G.A. Bain, A. E. Liberta, J.V. Martinez, S.H. Ortiz, R.A. Toscano, Polyhedron 14 (1995) 2189.
[41] M.L. Low, G. Paulus, P. Dorlet, R. Guillot, R. Rosli, N. Delsuc, K. Crouse, C. Policar, BioMetals (2015) 553.
[42] S.S. Konstantinović, B.C. Radovanović, A. Krklješ, J. Therm. Anal. 90 (2007) 525.
[43] R. Takjoo, R. Centore, M. Hakimi, S.A. Beyramabadi, A. Morsali, Inorganica Chim. Acta 371 (2011) 36.
[44] A.B.P. Lever, Inorganic Electronic Spectroscopy, second edition, (Amsterdam: Elsevier) (1986) 534.
[45] V. Suni, M.R.P. Kurup, M. Nethaji, Polyhedron 26 (2007) 3097.
[46] D.F. Evans, J. Chem. Soc. (1959) 2003.
[47] S.J. Coles, P.A. Gale, Chem. Sci. 3 (2012) 683.
[48] G.M. Sheldrick, Acta Cryst. A71 (2015) 3.
[49] O.V. Dolomanov, L.J. Bourhis, R.J. Gildea, J.A.K. Howard, H. Puschmann, J. Appl. Cryst. 42 (2009) 339.
[50] G.M. Sheldrick, Acta Cryst. C27 (2015) 3.
[51] W. Kaminsky, K.I. Goldberg, D.X. West, J. Mol. Struct. 605 (2002) 9.
[52] T.S. Gardner, F.A. Smith, E. Wenis, J. Lee, J. Org. Chem. 21 (1956) 530.